

Phenomenology of lepton-nucleus DIS

S. A. Kulagin^{a*} and R. Petti^{b c}

^a Institute for Nuclear Research, 117312 Moscow, Russia

^b CERN, CH-1211 Genève 23, Switzerland

^c University of South Carolina, Columbia SC 29208, USA

The results of recent phenomenological studies of unpolarized nuclear deep-inelastic scattering are discussed and applied to calculate neutrino charged-current structure functions and cross sections for a number of nuclei.

1. Introduction and motivations

Significant nuclear effects were discovered in charged-lepton (CL) deep-inelastic scattering (DIS) experiments (for a review see [1,2]). The experimental observations indicate that the nuclear environment plays an important role even at energies and momenta much larger than those involved in typical nuclear ground state processes. The study of nuclei is therefore directly related to the interpretation of high-energy experiments with nuclei from hadron colliders to fixed target experiments.

The understanding of nuclear effects is particularly relevant for neutrino processes in which weak interaction with matter requires the use of heavy nuclear targets in order to collect significant number of interactions. Therefore a reliable treatment of nuclear effects is important for interpretation of neutrino experiments and in some cases crucial for reducing systematic uncertainty.

In this paper we briefly review the results of recent studies of CL nuclear DIS of Ref.[3] and apply this approach to calculate the (anti)neutrino differential cross sections of charged-current (CC) interactions with nuclei.

2. Nuclear structure functions

The theoretical background of the analysis of Ref.[3] involves the treatment of a few different

mechanisms of nuclear effects which are characteristic for different kinematical regions. Summarizing, for the nuclear structure function of type $a = 1, 2, 3$ we have

$$F_a^A = F_a^{p/A} + F_a^{n/A} + F_a^{\pi/A} + \delta_{\text{coh}} F_a^A, \quad (1)$$

where $F_a^{p/A}$ ($F_a^{n/A}$) are the incoherent contributions from the bound protons (neutrons) corrected for Fermi motion, nuclear binding and off-shell effects (impulse approximation). The term $F_a^{\pi/A}$ is a correction associated with scattering off the nuclear pion (meson) field. The term $\delta_{\text{coh}} F_a^A$ is a correction due to coherent interaction of intermediate virtual boson with nuclear target.

The terms $F_a^{p/A}$ and $F_a^{n/A}$ are calculated as the proton and the neutron structure function averaged with the nuclear spectral function and corresponding kinematical factors. In particular, for $F_2^{p/A}$ we have²

$$F_2^{p/A}(x, Q^2) = \langle (1 + k_z/M) F_2^p(x', Q^2, k^2) \rangle, \quad (2)$$

where $k = (M + \varepsilon, \mathbf{k})$ and $x' = x/(1 + (\varepsilon + k_z)/M)$ are the four-momentum of bound proton and its Bjorken variable. The averaging is taken over the proton spectral function which describes the distribution of bound nucleons over momentum and energy. Similar expression holds for the neutron term.

²Eq.(2) is written for the kinematics of the Bjorken limit assuming that momentum transfer is along z axis $q = (q_0, 0_{\perp}, -|q|)$. For more general expressions valid at finite Q and further detail see Ref.[3].

*Supported in part by the Russian Foundation for Basic Research project 03-02-17177 and INTAS project 03-51-4007.

Nuclear Fermi motion and binding corrections provide a correct trend of observed behavior of the ratios $\mathcal{R}_2 = F_2^A/F_2^D$ (so-called EMC ratio) however the quantitative description of data is missing in impulse approximation. In a quantitative treatment it is important to go beyond this approximation and take into account that the structure functions of bound nucleons can be different from those of the free nucleons. In Ref.[3] this effect is modelled by off-shell corrections, i.e. the dependence of structure functions on k^2 in Eq.(2). Since characteristic energies and momenta of bound nucleons are small compared to the nucleon mass we treat off-shell effects as a linear correction in $k^2 - M^2$ to the structure function of the on-shell nucleon

$$F_2(x, Q^2, k^2) = F_2(x, Q^2) \left(1 + \delta f_2 \frac{k^2 - M^2}{M^2} \right). \quad (3)$$

The function $\delta f_2(x, Q^2)$ describes the relative off-shell effect. In analysis of Ref.[3] this function is treated phenomenologically. In particular, we assume δf_2 to be independent of Q^2 and parametrize its x dependence as

$$\delta f_2 = C_N(x - x_1)(x - x_0)(h - x), \quad (4)$$

where $0 < x_1 < x_0 < 1$ and $h > 1$.

It should be noted that because of binding the nucleons do not carry all of the light-cone momentum of the nucleus and the momentum balance equation is violated in the impulse approximation thus indicating the presence of non-nucleon degrees of freedom in the problem. In Ref.[3] we consider a correction to nuclear structure function due to scattering off meson fields in nuclei in the convolution approximation

$$F_2^{\pi/A} = \int_x dy f_{\pi/A}(y) F_2^\pi(x/y, Q^2), \quad (5)$$

where $f_{\pi/A}(y)$ is the distribution of nuclear pion excess in a nucleus and F_2^π is the pion structure function. The distribution function $f_{\pi/A}(y)$ is calculated using the constraints from equations of motion for interacting pion-nucleon system. By using the light-cone momentum balance equation we effectively constrain the contribution from all mesonic fields responsible for nuclear binding.

In the small- x region the coherent effects in DIS are relevant (for a review see Ref.[2]). These effects are associated with the fluctuations of intermediate virtual boson into quark-gluon (or hadronic) states. At small x an average time of life of such fluctuation is significantly larger than the average distance between bound nucleons. For this reason the virtual hadronic states undergo multiple nuclear interactions while traversing a nucleus that causes nuclear shadowing effect. The rate of this effect depends on the scattering amplitude of the virtual hadronic states off the nucleon. In our approach we model the interaction of virtual hadronic states with the nucleon as scattering of a single state with effective cross section $\bar{\sigma}$. In this approximation the relative nuclear correction to the structure function is determined by the corresponding correction to effective cross section $\bar{\sigma}$. In our studies [3] the effective cross section $\bar{\sigma}$ for the scattering off the nucleon is treated phenomenologically and parametrized as

$$\bar{\sigma} = \sigma_1 + \frac{\sigma_0 - \sigma_1}{1 + Q^2/Q_0^2} \quad (6)$$

where the parameters σ_0 and σ_1 describe low- Q and high- Q limits while the scale Q_0 controls transition region. The nuclear corrections to effective cross section were calculated using the Glauber–Gribov multiple scattering theory.

We used the outlined approach in the analysis of data on the ratios $\mathcal{R}_2(A/B) = F_2^A/F_2^B$ of structure functions of two nuclei. The general goal was to develop a quantitative model of nuclear structure functions which, from one side, would include the major mechanisms of nuclear scattering and, from the other side, would describe the existing data with acceptable accuracy. We analyze data on \mathcal{R}_2 for a variety of targets from D to Pb for a wide kinematical region (for more detail see Table 1 of Ref.[3]). From preliminary analysis of data we observed strong correlations between some of the model parameters. In order to reduce the number of free parameters we used additional constraints. In particular, the parameters h and x_0 turned out to be fully correlated and related as $h = 1 + x_0$. The parameter x_1 is strongly correlated with C_N and Q_0 . We

performed several fits with different fixed values of x_1 and found that $x_1 = 0.05$ corresponds to the lowest χ^2 and provides a good cancellation between shadowing and off-shell correction to the normalization of nuclear valence quark distribution. From preliminary fits the best fit value of σ_1 was consistent with zero and we fixed $\sigma_1 = 0$ in the final fit. The parameter σ_0 was fixed to 27 mb (averaged meson-nucleon total cross section in the vector meson dominance model [4,2]) in order to reproduce the photoproduction limit. The remaining parameters C_N , x_0 and Q_0 were adjusted to reproduce data. The global fit of Ref.[3] to all data results in $C_N = 8.1 \pm 0.3 \pm 0.5$, $x_0 = 0.448 \pm 0.005 \pm 0.007$, $Q_0^2 = 1.43 \pm 0.06 \pm 0.2 \text{ GeV}^2$ with $\chi^2/\text{d.o.f.} = 459/556$ (the last error is the estimate of systematic or theoretical uncertainty). In order to test the model we performed a number of fits to different sub-sets of nuclei in the region from ${}^4\text{He}$ to ${}^{208}\text{Pb}$. The results are compatible within the uncertainties with the result of the global fit thus indicating an excellent consistency between the model and the data for all nuclei.

3. Neutrino-nucleus inelastic cross sections

In this paper we apply the developed model of nuclear structure functions to calculate the differential cross sections of (anti)neutrino inelastic scattering. In contrast to the CL scattering, which is driven by electromagnetic interaction, neutrino interactions are characterized by the presence of both the vector current (VC) and the axial current (AC) contributions. The VC-AC interference gives rise to P-odd and C-odd terms in the cross section which are described by the structure function F_3 , which is absent in CL scattering. In contrast to VC the AC is not conserved. For this reason the AC contribution plays important role and even dominates the (anti)neutrino cross sections at low Q . In this region the terms due to non conservation of the AC are most important for the longitudinal structure function F_L which is determined by the divergence of the current (Adler theorem [5]). At low momentum transfer the divergence of the AC is dominated by the pion field (PCAC) that al-

lows us to calculate the leading term at low Q^2 : $F_L^{\text{PCAC}} = f_\pi \sigma_\pi(s, Q^2)/\pi$, where $f_\pi = 0.93 m_\pi$ is the pion decay constant and σ_π is the total pion-nucleon (nucleus) cross section with the center-of-mass energy squared $s = M^2 + Q^2(1/x - 1)$. It should be also noted that σ_π describes interaction of an off-shell pion with momentum q and the virtuality $-Q^2$. Although the contribution from the VC to F_L vanishes at low Q^2 , it rises with Q^2 and has to be taken into account at $Q^2 \sim 1 \text{ GeV}^2$ as well as for higher values of momentum transfer. We explicitly separate the PCAC term and write the full F_L as

$$F_L(x, Q^2) = F_L^{\text{PCAC}} f_{\text{PCAC}}(Q^2) + \tilde{F}_L(x, Q^2), \quad (7)$$

where \tilde{F}_L incorporates the contributions from VC and non-PCAC terms from AC which vanish at $Q^2 \rightarrow 0$. In order to interpolate between low and high Q^2 we introduced a form factor $f_{\text{PCAC}} = (1 + Q^2/M_{\text{PCAC}})^{-2}$, where M_{PCAC} represents the scale controlling the PCAC contribution. Since the pion pole does not contribute to the structure functions (because of transversity of the lepton current, see Ref.[6] and references therein) the scale M_{PCAC} is not determined by the pion mass but rather related to higher mass states like a_1 meson and $\rho\pi$ continuum.³ The term \tilde{F}_L dominates at high Q^2 at which it is identified with the pQCD structure function with target mass (TMC) and higher twist (HT) corrections. In numerical applications we use the PDFs and HT of Ref.[7] which were derived from the analyses of CL DIS data. In order to evaluate \tilde{F}_L at low values of Q^2 we apply polynomial extrapolation between pQCD calculation at high Q^2 and the limit of $Q \rightarrow 0$ with the matching point at $Q^2 = 1 \text{ GeV}^2$ [8].

The magnitude and the Q^2 dependence of the PCAC term in F_2 is illustrated in Fig. 1. Note that the magnitude of the PCAC term decreases for heavy nuclei because of the nuclear shadowing effect for the pion cross section.

It is also important to note that for neutrino scattering the PCAC term leads to the rising ratio

³In numerical calculations described below we used $M_{\text{PCAC}} = m_{a_1}$. In Ref.[6] it was argued that the relevant scale is given by the $\rho\pi$ cut rather than the a_1 pole. However, both values are close numerically.

$R = F_L/F_T$ at low Q^2 in contrast to the CL case. This effect is illustrated in Fig. 2 where $R(Q^2)$ was calculated for two fixed values of x for the isoscalar nucleon (average over the proton and the neutron) and a number of nuclei [8,9].

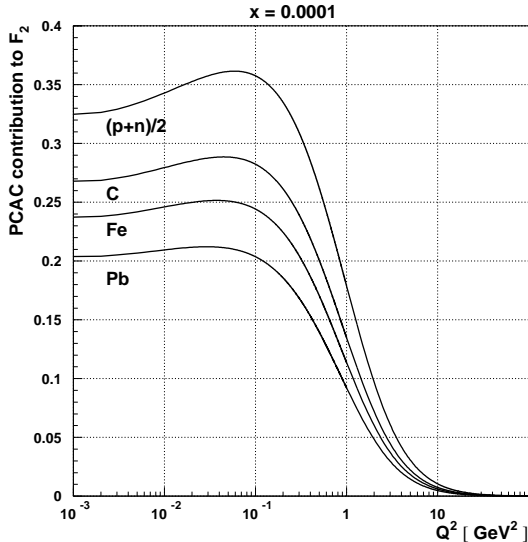


Figure 1. The PCAC term in neutrino F_2 calculated as a function of Q^2 for the fixed $x = 0.0001$ [9]. The results are shown for the isoscalar nucleon (average over the proton and the neutron) and for ^{12}C , ^{56}Fe and ^{208}Pb nuclei.

In Figures 3, 4 and 5 we report the results of our calculations of (anti)neutrino differential cross sections in comparison with the measurements for several values of the (anti)neutrino energy from 20 GeV to 170 GeV [9]. The calculation of (anti)neutrino nuclear structure functions uses the same NNLO PDFs and HT terms obtained from the analyses of charged-lepton DIS data [7] and which were applied in the analysis described above. The treatment of nuclear effects is based on the results of Ref.[3]. In the calculations we used the off-shell function δf_2 , derived from CL data in Ref.[3], for both F_2 and F_3 for neutrino and antineutrino. Nuclear effects in the

PCAC term are controlled by the multiple scattering corrections to the pion cross section σ_π . We also remark that nuclear pion excess correction (Eq.(5)) vanishes for F_3 . As a result, we observe a good agreement between the data and our calculations for all examined nuclei that provides a good test of the model of Ref.[3]. It should be noted that the data points at low x bins, which typically have low Q^2 (for example for CHORUS data $Q^2 \sim 0.25 \text{ GeV}^2$), are also reproduced by calculation. In this region the cross sections are dominated by the PCAC term. Thus our analysis supports the presence of significant PCAC effects in neutrino inelastic scattering at $Q^2 \gg m_\pi^2$.

Acknowledgments

S.K. is grateful to the organizers of the NuInt05 for support and hospitality.

REFERENCES

1. M. Arneodo, Phys. Rept. **240**, 301 (1994).
2. G. Piller and W. Weise, Phys. Rept. **330**, 1 (2000) [arXiv:hep-ph/9908230].
3. S. A. Kulagin and R. Petti, Nucl. Phys. A **765** (2006) 126 [arXiv:hep-ph/0412425].
4. T. H. Bauer, R. D. Spital, D. R. Yennie and F. M. Pipkin, Rev. Mod. Phys. **50**, 261 (1978) [Erratum-ibid. **51**, 407 (1979)].
5. S. L. Adler, Phys. Rev. **135** (1964) B963.
6. B. Z. Kopeliovich, Nucl. Phys. Proc. Suppl. **139** (2005) 219 [arXiv:hep-ph/0409079].
7. S. I. Alekhin, Phys. Rev. D **68**, 014002 (2003), [arXiv:hep-ph/0211096].
8. S. I. Alekhin, S. A. Kulagin and R. Petti, in preparation.
9. S. A. Kulagin and R. Petti, in preparation.
10. R. Petti, this Proceedings.
11. G. Onengut *et al.* [CHORUS Collaboration], Phys. Lett. B **632** (2006) 65.
12. M. Tzanov [NuTeV Collaboration], arXiv: hep-ex/0507040.

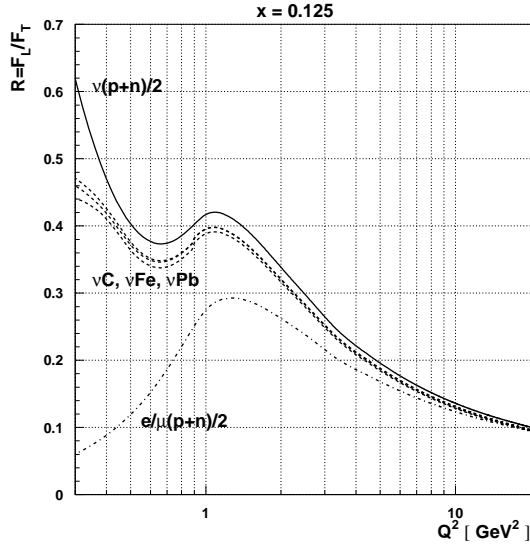
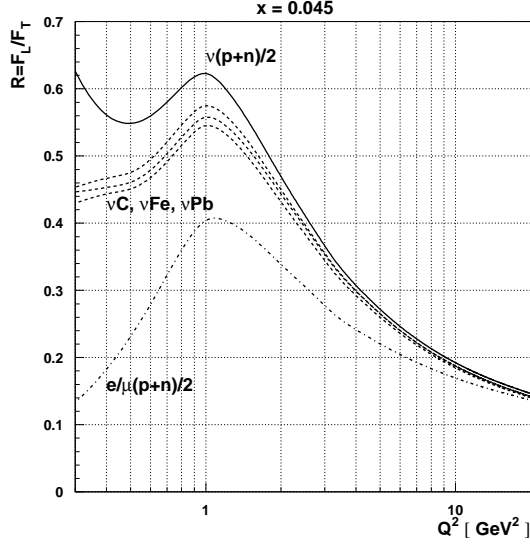


Figure 2. Comparison of the ratio $R = F_L/F_T$ calculated for charged leptons (dashed-dotted) and neutrino (solid) for the isoscalar nucleon as a function of Q^2 at $x = 0.045$ (upper panel) and $x = 0.125$ (lower panel). Also shown are the results of calculation of R for neutrino scattering off ^{12}C , ^{56}Fe and ^{208}Pb (from top to bottom).

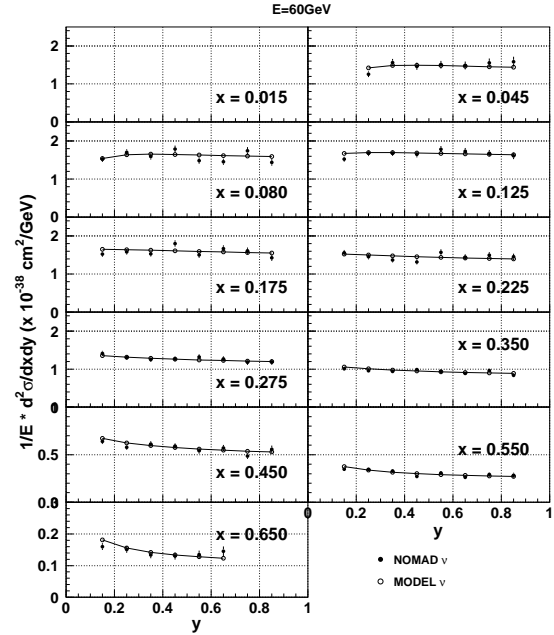
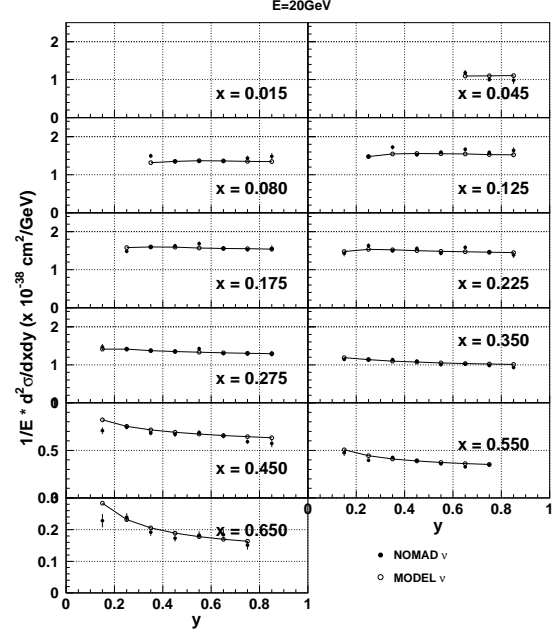


Figure 3. Comparison of our calculations (open symbols) with NOMAD data [10] (full symbols) for neutrino differential cross-sections on ^{12}C at $E = 20$ GeV (upper panel) and $E = 60$ GeV (lower panel).

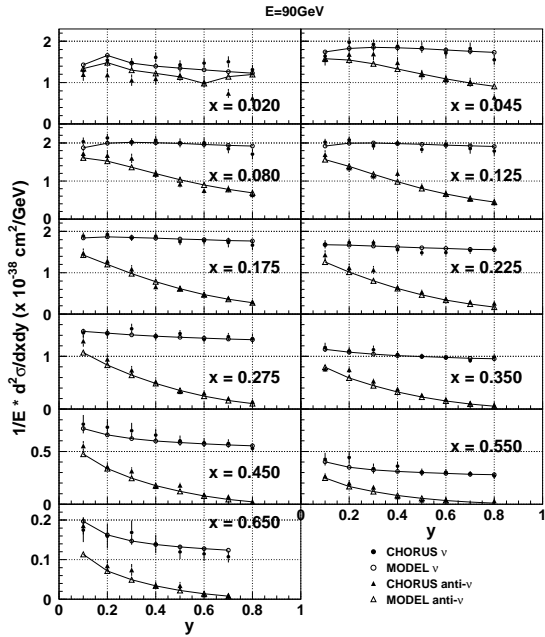
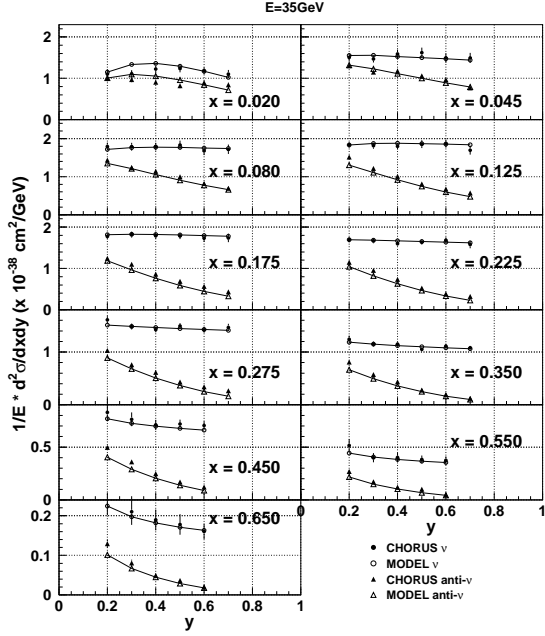


Figure 4. Comparison of our calculation (open symbols) with CHORUS data [11] (full symbols) for neutrino (circles) and antineutrino (triangles) differential cross-sections on ^{207}Pb at $E = 35\text{ GeV}$ (upper plot) and $E = 90\text{ GeV}$ (lower plot).

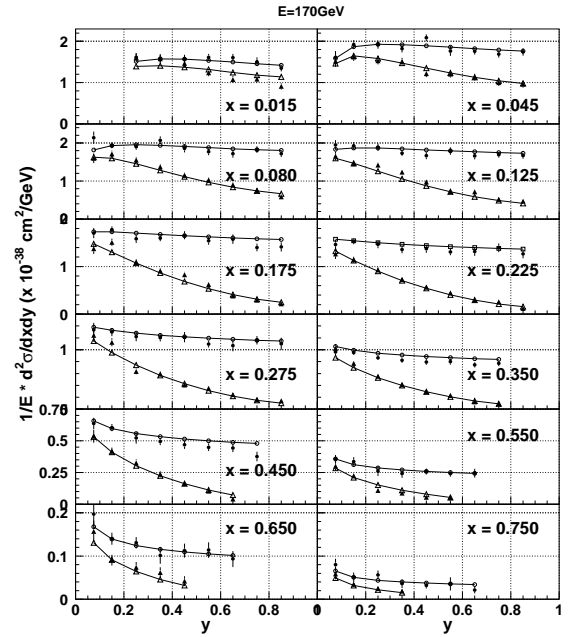
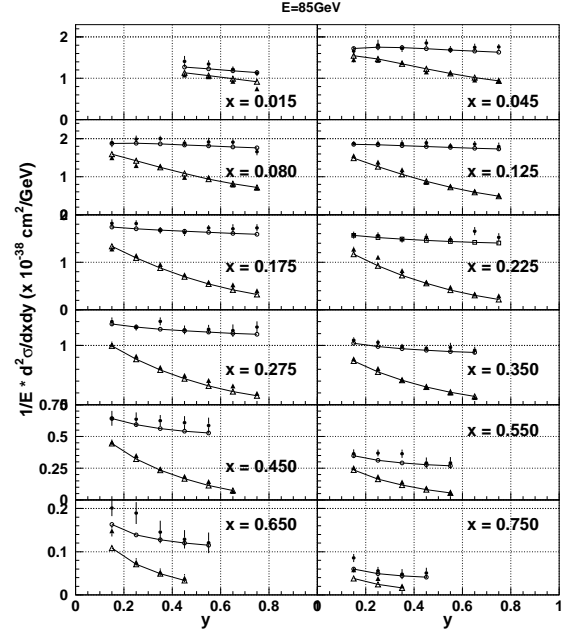


Figure 5. Comparison of our calculation (open symbols) with NuTeV data [12] (full symbols) for neutrino (circles) and antineutrino (triangles) differential cross-sections on ^{56}Fe at $E = 85\text{ GeV}$ (upper plot) and $E = 170\text{ GeV}$ (lower plot).